

Surface Energy Budget at Amdo on the Tibetan Plateau using GAME/Tibet IOP98 Data

By Kenji Tanaka

*Department of Civil and Environmental Engineering, Faculty of Engineering, Kumamoto University,
Kumamoto, Japan*

Hirohiko Ishikawa, Taiichi Hayashi

Disaster Prevention Research Institute, Kyoto University, Kyoto, Japan

Ichiro Tamagawa

Department of Civil Engineering, Faculty of Engineering, Gifu University, Gifu, Japan

and

Yaoming Ma

Cold and Arid Regions Environmental and Engineering Research Institute, CAS, China

(Manuscript received 4 February 2000, in revised form 24 October 2000)

Abstract

In the east of Tibetan Plateau, Amdo, the surface energy flux measurement with eddy correlation technique was conducted during the Intensive Observation Period (IOP) of GEWEX Asian Monsoon Experiment (GAME). This study is a preliminary analysis on surface energy budget at Amdo with these data.

There is a remarkable change in sensible and latent heat fluxes between pre-monsoon season and summer monsoon season. In the pre-monsoon, the ground surface and the surface layer were very dry. The specific humidity was 2 to 4 g/kg and the sensible heat flux was dominant. As the monsoon progresses, the surface becomes wet due to almost daily precipitation. Accordingly, the sensible heat flux decreases and the latent heat flux increases. In the beginning of September, nearly the end of the summer monsoon, the latent heat flux exceeds the sensible heat flux.

The ground heat flux at the surface was estimated using the observed soil temperature profile with the aid of the thermal conductive equation. The computed ground heat flux corresponds to the residual of the surface energy balance in the daytime. But disagreement occurred in the evening, when the surface temperature rapidly decreases. On the daily averaged bases, the surface energy balance is not well closed. In terms of closure ratio, the value in a typical clear day was 67%. Another rough estimation of soil heat flux is made, in which the heat needed to melt the soil water and to heat up the soil layer was calculated. According to this, it was estimated that about 30 W/m² (20% of net radiation) of soil heat flux was required on average over April 20 to July 20, but the measured soil heat flux was only 5.7 W/m².

Corresponding author: Kenji Tanaka, Department of Civil and Environmental Engineering, Faculty of Engineering, Kumamoto University, Kumamoto 860-0862, Japan
E-mail: ktanaka@gpo.kumamoto-u.ac.jp
©2001, Meteorological Society of Japan

1. Introduction

The GEWEX (Global Energy and Water cycle Experiment) Asian Monsoon Experiment (GAME) started in 1996. The Tibetan Plateau is one of

the major experimental regions of the GAME. It is in the midlatitude ($29^{\circ}\sim 38^{\circ}\text{N}$) of the eastern Eurasian continent ($80^{\circ}\sim 100^{\circ}\text{E}$), where the averaged altitude is more than 4,500 m, and it covers about 1.2 million km^2 area.

Tibetan Plateau has been thought to play a very important role in the progress of Asian monsoon, as discussed by many authors. The impact of the Plateau on the surrounding region has been discussed for its orographic effect and for the thermal effect as an elevated heat source (or sink) in the midtroposphere. The Plateau blocks the tropospheric circulation, and contributes to the development of the monsoon circulation in summer and the formation of the Siberian high-pressure system in winter (e.g., Manabe and Terpsta 1974). The surface of the Plateau is strongly heated by incoming solar radiation in daytime (and cooled in the night by strong longwave radiation), so that the air over the Plateau is relatively warmer (or cooler) than that of surrounding air at same altitude. Flohn (1959) discovered the high temperature anomaly at 500 hPa level over the Plateau. Thus, it is important to estimate the heat flux from the plateau surface to the atmosphere to understand the mechanism of energy cycle over Asian Monsoon region.

Before the GAME/Tibet, the First Global Atmospheric Research Program (GARP) Global Experiment (FGGE) (e.g., Yeh and Gao 1979) and the Chinese Qinghai-Xizhang Plateau Meteorology Experiment (QXPME) were conducted (e.g., Johnson et al. 1987; Yeh 1988; Zhang et al. 1988; Ji et al. 1989). With these data several indirect methods have been employed to estimate surface energy fluxes by Chinese scientists. Gao and Liu (1984) and Zhang et al. (1988) estimated the surface flux using Bowen Ratio Technique. The surface heat and moisture fluxes were also estimated indirectly with the use of the upper-air observation data. In this, both sensible and latent heat fluxes were estimated as the residual of the vertically integrated heat or moisture budget equation. Li and Yanai (1992) reviewed those studies and summarized that they had demonstrated the presence of positive temperature anomalies over the Tibetan Plateau and the large-scale vertical circulation induced by the plateau throughout the nine months from winter to summer, and that before the onset of the summer monsoon, the heat source on the plateau was surrounded by intense cooling in the adjacent regions.

Although these previous studies have unveiled

the features and the roles of the plateau boundary layer to a considerable extent, present knowledge is not enough to contribute to the development of prognostic model for the land-atmosphere processes over the Plateau. In the GAME/Tibet, an intensive observation of land surface-atmosphere interaction was conducted at a site called Amdo. In addition to the conventional wind-, temperature- and humidity-profiles and radiation measurements, the atmospheric turbulence was measured almost continuously for about 4 months, from late May to early September in the summer of 1998. This turbulence measurement provides the eddy sensible and latent fluxes, which are probably the first attempt to estimate the sensible and latent heat fluxes 'directly' over the plateau.

In this paper, using the data obtained at Amdo during the GAME/Tibet IOP, preliminary analysis on surface energy budget is presented. The sensible heat and the latent heat fluxes are directly obtained from the eddy correlation method. The soil heat flux is estimated from the data of the soil layer observation.

The instrumentation of planetary boundary layer observation is described in section 2. General features of the meteorology are introduced in section 3. In section 4, the typical diurnal changes of the surface energy budget are introduced first. Then, the surface energy balance is discussed. In this section, an attempt of ground heat flux estimation using the near surface soil temperature and moisture data is also presented. In section 5, we summarize this study.

2. Instrumentation

Amdo is located on the eastern Tibetan Plateau along the Xisang-Qinghai highway (Figure 1). The site ($31^{\circ}14.468'\text{N}$, $91^{\circ}37.507'\text{E}$) is about 6 km west of the town of Amdo. The altitude is about 4800 m. The surface is almost bare soil in the pre-monsoon dry season, but is covered with scattered short grasses during summer monsoon season. The following observation facilities were installed at the site.

2.1 PBL-tower measurement

A fourteen-meter tower was set up to measure the temperature, humidity and wind profiles in the surface layer. The MILOS500 system of VAISALA was used to collect and record the data. In addition these profiles atmospheric pressure, precipitation, and soil parameters were also measured by this system. Their ten-minute averages were stored

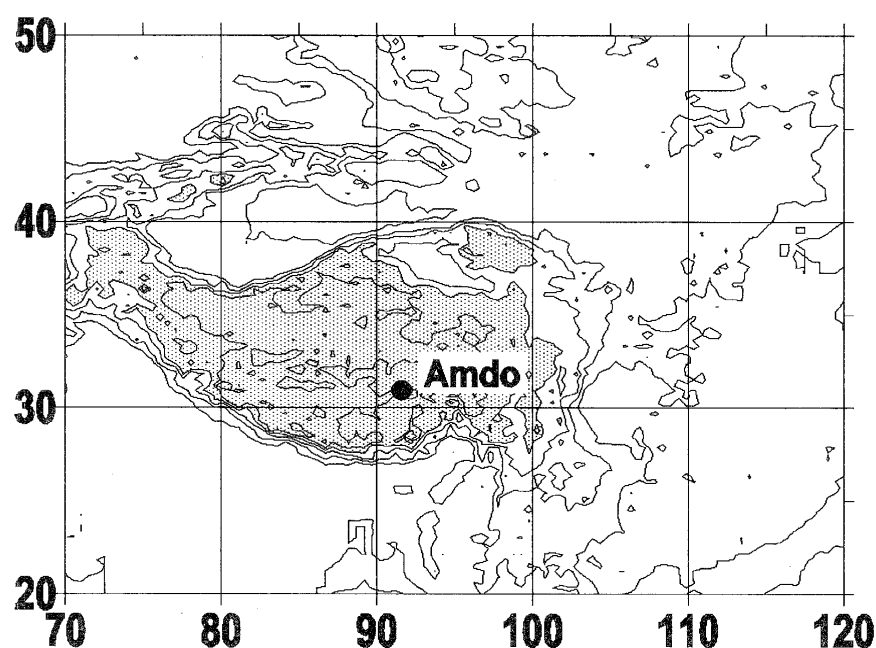


Fig. 1. Location of Amdo. The area higher than 4000 m is hatched.

Table 1. The sensors of 14 meter tower measurement.

Variable	Level (m)	Sensor
Wind	1.9, 6.0 and 14.1	Aerobane(OGASAWARA FF-11)
Temperature	1.55, 5.65 and 13.75	Pt-100(VAISALA HMP35D)
Humidity	1.55, 5.65 and 13.75	Electric Capacitance(ibid)
Pressure	-----	Semi-conductor(VAISALA DPA21)
Precipitation	-----	Tipping bucket(VAISALA RG-13)
Surface temperature	-----	IR thermometer(Optex HR1-FL)
Soil temperature	0.05, 0.1, 0.2 and 0.4	Pt-100
Soil heat flux	0.1 and 0.2	Heat plate(EKO MF-81)

consequently. The sensors used in the system are listed in Table 1.

2.2 Radiation

Four components of radiation, upward and downward fluxes of short wave and long wave radiation, were measured and recorded by an independent system. The sensors used were EKO MS-801 (short wave radiation) and Eppley PIR (long wave radiation). In measuring the long wave radiation, the dome and the base temperatures of each ra-

diometer were also measured for correction with secondary long wave emission from the dome of sensor (Shimura 1996). A data logger (VAISALA, QLC50) sampled the data every second and the 10-minutes averages were recorded in it. In order to synthesize the logger clock with that of the tower system, the data of downward short wave radiation from both systems were used.

2.3 Turbulent flux measurement system

The turbulent flux measurement system was com-

posed of a sonic anemo-thermometer (DAT-300, Kaijo) and an infrared hygrometer (AH-300, Kaijo). A clinometer was also used to measure sensor inclination. The infrared hygrometer was used to detect the high frequency fluctuation. A capacity-type hygrometer and thermometer (Pt-100) were also set near the infrared hygrometer, and used to measure the low frequency fluctuation of the specific humidity. The sensor assembly was set up on the top of a pole (sensor height is about 2.8 m) about 20 m from the tower. The data were sampled in 10 Hz and recorded in magnetic optical disks. During the IOP, more than 4800 thirty-minute data were obtained.

The sensible heat flux (H) and the latent heat (lE) flux were calculated as,

$$H = \bar{\rho} \bar{C}_p \overline{w'T'}, \quad (1)$$

$$lE = -\bar{\rho} \overline{lw'q'}, \quad (2)$$

where \bar{C}_p and $\bar{\rho}$ are the specific heat and the density of moist air, w the vertical velocity, T the temperature, q the specific humidity and l the latent heat of water (2.5×10^6 J/kg). The dash represents the

fluctuation of the variable, and the over bar represents averaged value in processing unit (30 minutes, 18000 data in one run). Several corrections are included in the calculation. The detail of the data procession is described in Tamagawa (2000).

3. Results

3.1 Tower data

The measured meteorological variables are shown in Figure 2. It is seen that the rain started in the middle of June. Unfortunately, the tower data failed at the start of the monsoon during 6–15 June. Before the onset of monsoon, the specific humidity was ranged from 2–4 g/kg, but after that it increased to 8–10 g/kg. The surface temperature, which is computed from the upward and downward long wave radiations assuming the surface emissivity ($\varepsilon = 0.98$), has a remarkable feature. The diurnal variation is as large as 50 °C before the monsoon, but it reduces to about 20 °C after the onset of monsoon. In the wind velocity large diurnal variations also exist before the onset of monsoon, but the range of variation also reduces after the on set

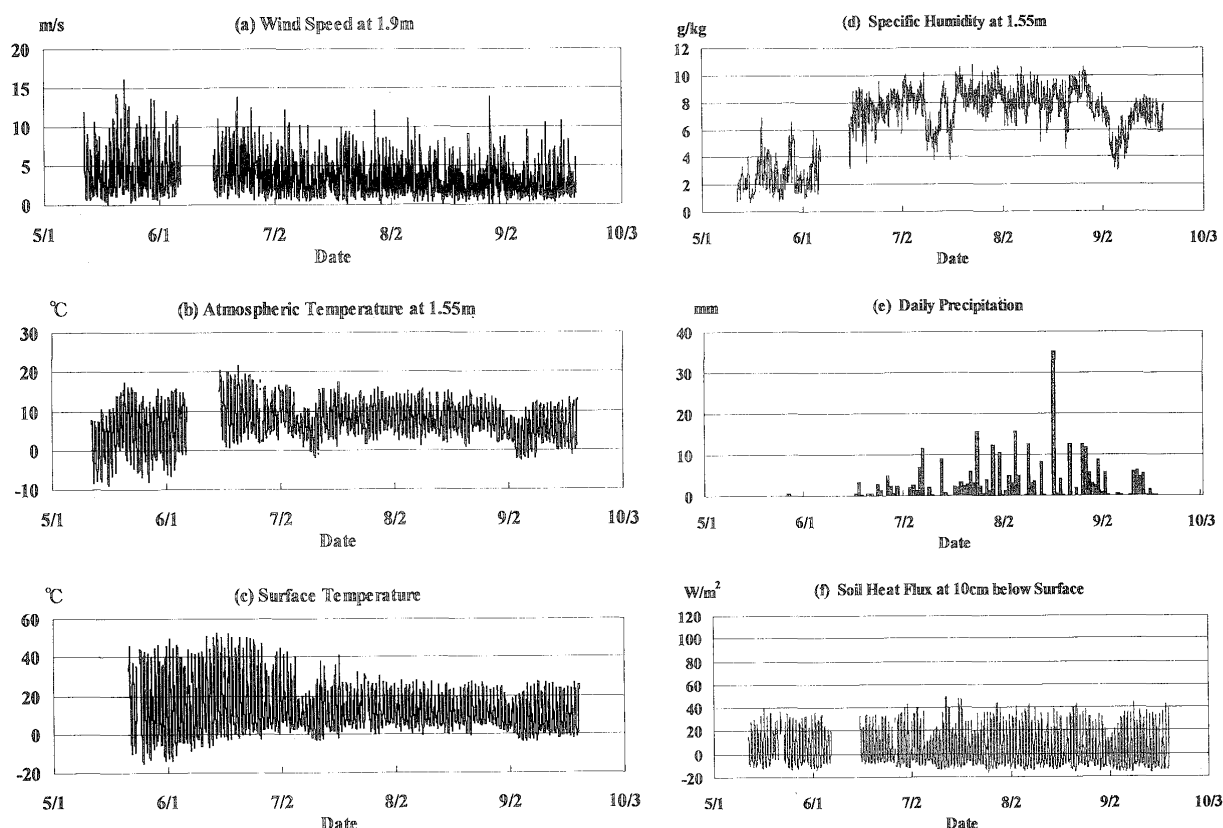


Fig. 2. Some meteorological variables observed at Amdo on GAME/Tibet during IOP (May 11–Sep. 20, 1998), obtained from PBL tower measurement except (c). (a) Wind speed at 1.9 m, (b) Atmospheric temperature at 1.55 m, (c) Surface Temperature calculated from long wave radiation, (d) Specific humidity, (e) Daily precipitation and (f) Soil heat flux at 10 cm below surface.

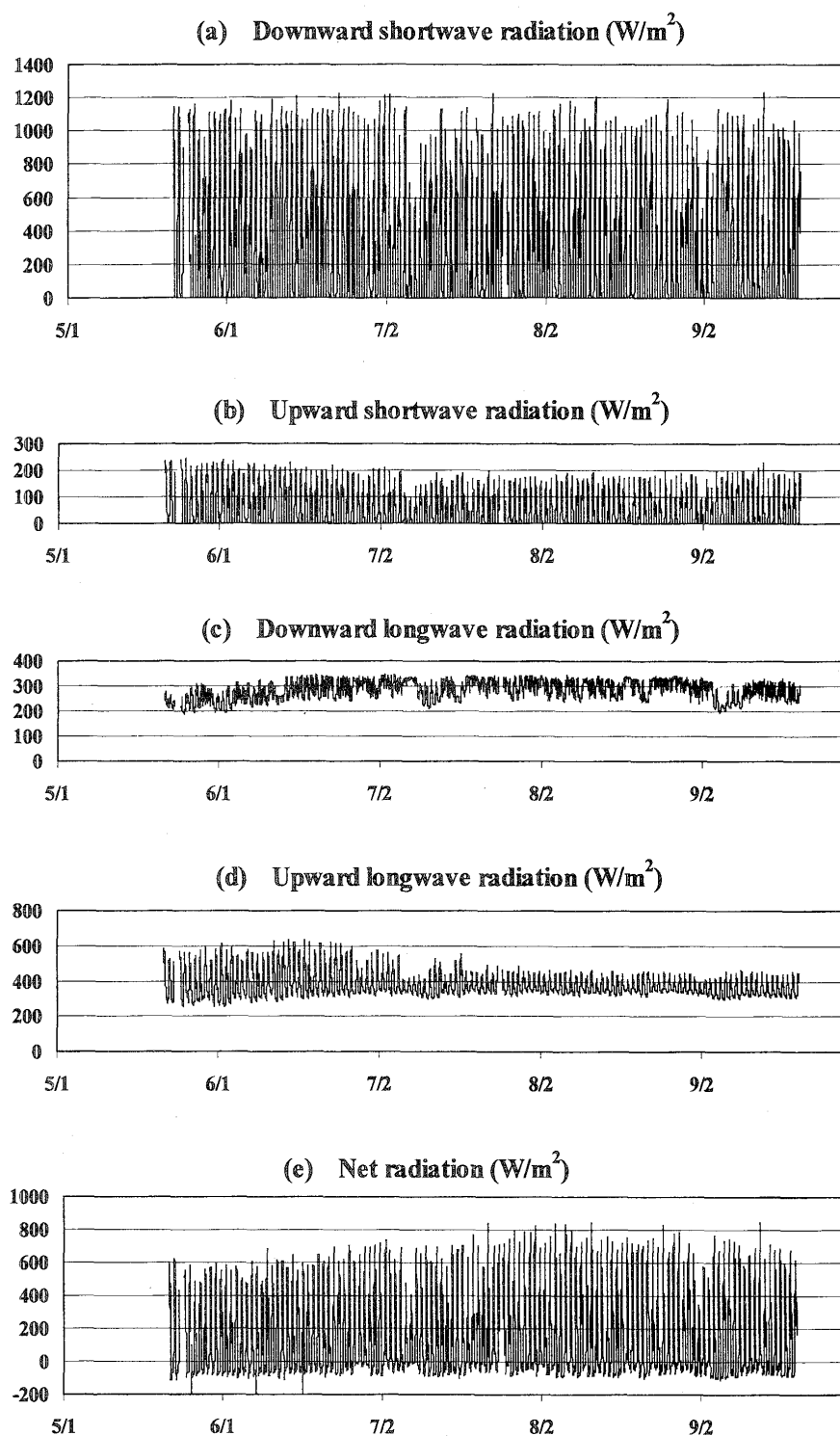


Fig. 3. Radiation fluxes observed at Amdo. Each panel shows (a) downward shortwave radiation, (b) upward shortwave radiation, (c) Downward longwave radiation, (d) upward longwave radiation, and (e) the net radiation.

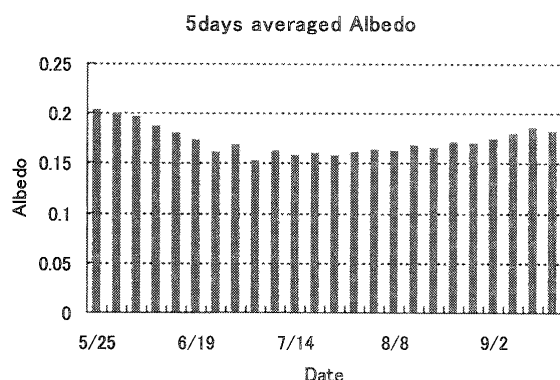


Fig. 4. Seasonal change of Albedo (as 5-days averaged value) during IOP, 1998.

of monsoon.

3.2 Radiation

Figure 3 shows all the recorded data of each radiation component and net radiation. The downward short wave radiation (*DSW*, Figure 3(a)) reaches about $1,100 \text{ W/m}^2$ at local noon on fine days in summer. The transmission rate of incoming solar radiation from the top of the atmosphere was estimated as about 85% in cloudless conditions. The value is about 10–15% greater than that observed

at the typical sea level station. This is due to the high altitude of the site, thus a shallower atmospheric layer between the top of the atmosphere and the ground surface.

On the other hand, the downward longwave (*DLW*, Figure 3(c)) marks in $250 \text{ W/m}^2 \sim 350 \text{ W/m}^2$. Higher *DLW* values more than 300 W/m^2 might result from the emission from clouds. Under clear sky conditions, *DLW* was about 50 W/m^2 smaller than that observed at a typical sea level site.

The upward short wave (*USW*, Figure 3(b)) is dependent on surface albedo. Figure 4 shows the 5-day averaged surface albedo. The averaged albedo decreased from about 0.20 to about 0.15 during June and July, due to the increase of the surface wetness and the growth of the grass.

The upward long wave (*ULW*, Figure 3(d)), equivalent to the surface temperature, varies diurnally more than 300 W/m^2 in the pre-monsoon season, but the diurnal amplitude of *ULW* decreases to less than 150 W/m^2 as the summer monsoon progresses.

The net radiation balance is shown in Figure 3(e). As the whole, strong short wave irradiation and long wave emission characterize the plateau

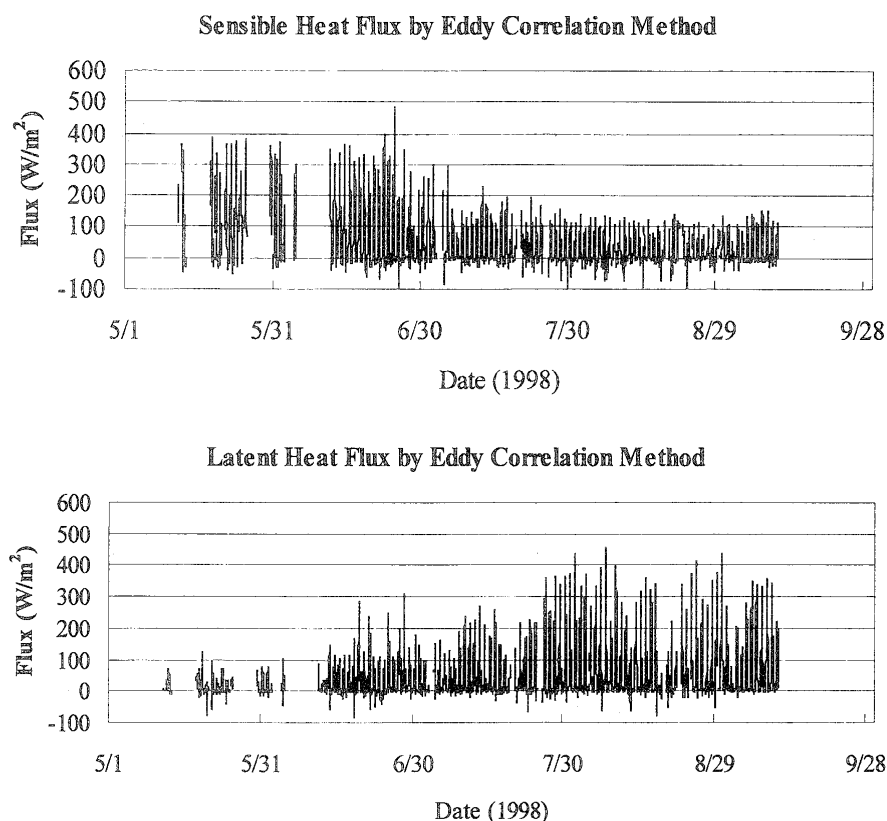


Fig. 5. Sensible heat flux and latent heat flux obtained by eddy correlation method.

radiation balance in the pre-monsoon season. In summer monsoon season, the reduced short wave irradiation seems to be compensated by reduced long wave emission, so that no remarkable distinction can be seen in the radiation budget between the pre-monsoon and monsoon seasons.

3.3 Turbulent flux

All data of sensible and latent heat fluxes are plotted in Figure 5. In pre-monsoon season, before the middle of June, the sensible heat flux reaches 400 W/m^2 in the daytime, nearly 10 times greater than the latent heat flux. As summer monsoon progresses, the latent heat flux increases gradually nearly 300 W/m^2 , but the sensible heat flux decreases and falls to 150 W/m^2 at daily maximum. Such a gradual change of these two fluxes matches well with the surface temperature change, specific humidity, etc. (see Figure 2). During the night, the sensible heat flux was downward. A strong downward sensible heat flux ($\sim 100 \text{ W/m}^2$) was calculated occasionally. Seeing the raw record, this corresponds to intermittent turbulence under very stable condition. However, the adequacy of the computed values are somewhat questionable. It should be noted that the power of IR source was suddenly weakened on August 17. And the lamp was replaced on August 23. Thus, the latent heat flux is unreliable during August 17–23. Also, the precipitation degrades the quality of measurement of both the SAT and IR hygrometer.

From the data presented in Figures 2 to 5, a change of surface climate can be seen in the middle of June, i.e., the onset of summer monsoon. Before the onset, the diurnal change of the surface temperature reaches 50°C , which contributes to the great sensible heat flux. After the onset of monsoon, the near surface soil moisture gradually becomes wet, due to the frequent precipitation. As the near surface soil moisture increases, both the latent heat flux and the soil heat capacity also increase. Thus, rising surface temperature is restricted and the sensible heat flux becomes lower (Figure 2(c)).

4. Discussion

4.1 Diurnal change of surface energy budget on typical clear sky days

In this section diurnal change of surface energy budget at typical sunny days are discussed with reference to the simplest form of surface energy balance (SEB) equation;

$$Rn - G_{sfc} = H + LE. \quad (3)$$

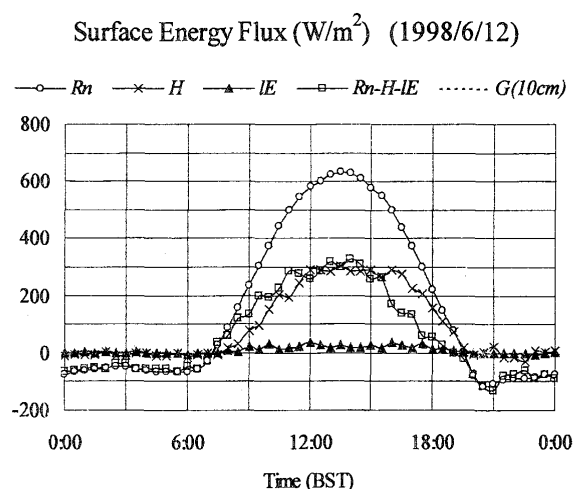


Fig. 6. The diurnal change of surface energy fluxes, on 1998/6/12, the pre-monsoon fine condition. *Rn*: net radiation flux, *H*: sensible heat flux, *LE*: latent heat flux and *Rn-H-LE*: the residual. BST represents Beijing Standard Time.

where G_{sfc} is the ground diffusive heat flux at surface.

Figure 6 shows the diurnal change of surface energy flux on June 12, 1998 as a case of pre-monsoon. In the morning, as the sun rises at about 0730 BST (Beijing Standard Time), net radiation flux increases rapidly. The sensible heat flux starts to increase at 1 hour after the sunrise, when the net radiation becomes positive. The sensible heat flux had its maximum value of about 300 W/m^2 at 1330 BST, about 47% of net radiation flux. On the other hand, the latent heat flux holds less than 40 W/m^2 , about 6% of net radiation. The reason is that the

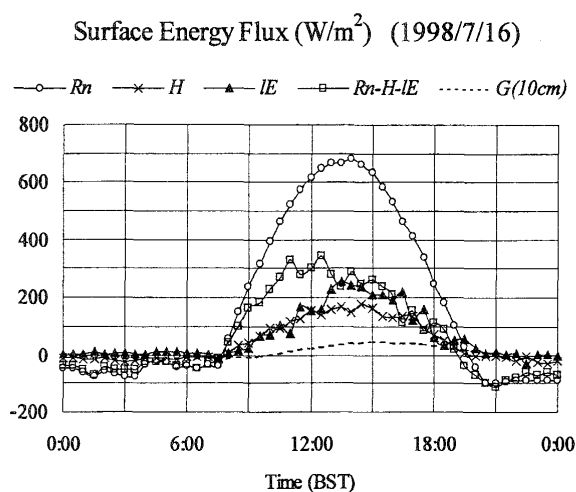


Fig. 7. Same as to Figure 6 but for July 16, 1998. Soil heat flux at 10 cm depth is also plotted.

near surface soil is very dry on that day: the volumetric soil water content is about $0.17 \text{ m}^3/\text{m}^3$ at 4 cm below surface. The residual flux holds nearly 50% of net radiation, about 320 W/m^2 at the maximum. This flux should be balanced by the ground diffusive heat flux.

Figure 7 shows the diurnal change of surface energy flux on July 16, 1998. This was the only day when cloud free sky prevailed throughout the daytime during the mid-monsoon. (During summer monsoon, cumulus cloud covered the sky in the afternoon almost every day, which brought some precipitation.) Both the sensible and latent heat fluxes start to increase when the net radiation becomes positive. During the daytime the sensible heat flux holds about 20~25% of the net radiation, and has the maximum value of 180 W/m^2 . The latent heat flux is about the same as the sensible

heat flux in the morning. After 1200 BST, however, the latent heat flux continues to increase to about 250 W/m^2 , while the sensible heat flux sustains the value at 1200BST.

Figure 8 shows the case of September 5, 1998. The sensible heat flux started to increase about one hour after the net radiation became positive. The latent heat flux began to increase at 0830, but fell down to 0 again at 0930, and started to increase again at 1030. The surface temperature, atmospheric temperature, soil temperature (10 cm) and atmospheric specific humidity of the day are plotted in Figure 9. The surface temperature was below 0°C in the early morning and rose up to 0°C in 0930 BST. The specific humidity held nearly constant between 0800~1000 then started to increase. Therefore, the complicated behavior of sensible and latent heat fluxes seem to relate to the melting of near surface frozen water.

In each of the three cases above, the residual flux reaches 300 W/m^2 in the daytime maximum. The reported typical value of the ground heat flux at a bare soil surface is 100 W/m^2 , about 8~15% of the net radiation in the daytime (see, e.g. Betts and Ball 1998; Garatt 1993). The soil heat flux measured by a heat panel at 10 cm below the surface ranges only between $-30\sim 60 \text{ W/m}^2$. If we assume the surface energy balance, the heat storage of near surface soil layer (from the surface to the 10 cm depth) must amount to 250 W/m^2 in the maximum, which seems extraordinary. In the next section, the ground diffusive heat flux at surface is estimated with the near surface soil temperature profile, in order to discuss the possibility of such a large heat flux into soil.

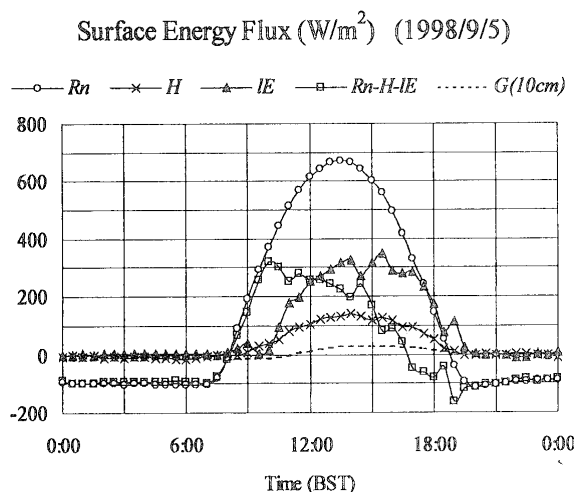


Fig. 8. Same as Figure 6 but for September 5, 1998.

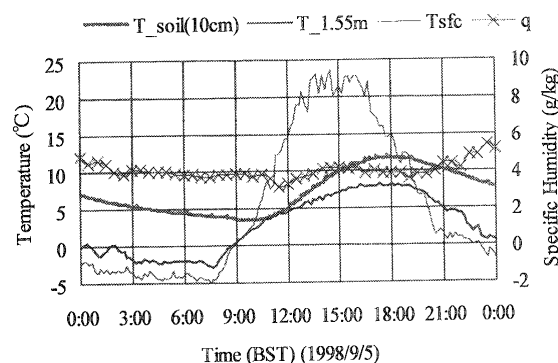


Fig. 9. Soil temperature (10 cm), air temperature (1.5 m), ground surface temperature, and specific humidity (1.5 m) on September 5, 1998.

4.2 Ground diffusive heat flux (G_{sfc})

The ground diffusive heat flux (G_{sfc}) is difficult to measure directly. G_{sfc} can be estimated indirectly from the soil temperature (and moisture) profile. In this study, G_{sfc} is computed from the following equation,

$$G_{sfc} = G_z + \int_0^z C_s \frac{\partial T}{\partial t} dz, \quad (4)$$

where C_s (J/m^3) is the volumetric heat capacity, and G_z is the observed soil heat flux below z from the surface ($z = 10 \text{ cm}$ was taken here).

The heat capacity of soil is given simply as,

$$C_s = (1 - \eta_{sat})\rho_d c_d + \eta_w \rho_w c_w, \quad (5)$$

where the first term of right hand side of Eq.(5),

Table 2. Soil parameters as a function of Elven USDA (United State Department of Agriculture, 1951) textual classes plus peat.

Soil Type	η_{sat} (m ³ /m ³)	Ψ_{sat} (m)	b	$(1-\eta_{sat})\rho_d c_d$ (MJ/m ³ K)
Sand	0.395	-0.121	4.05	1.47
Loamy Sand	0.410	-0.090	4.38	1.41
Sandy Loam	0.435	-0.218	4.90	1.34
Silt Loam	0.485	-0.786	5.30	1.27
Loam	0.451	-0.478	5.39	1.21
Sandy Clay Loam	0.420	-0.299	7.12	1.18
Silty Clay Loam	0.477	-0.356	7.75	1.32
Clay Loam	0.476	-0.630	8.52	1.23
Sandy Clay	0.426	-0.153	10.40	1.18
Silty Clay	0.492	-0.490	10.40	1.15
Clay	0.482	-0.405	11.40	1.09
Peat	0.863	-0.356	7.75	0.84

$(1 - \eta_{sat})\rho_d c_d$, represents the volumetric heat capacity of soil under dry condition. And η_w , ρ_w , and c_w represent the volumetric soil water content, the density of liquid water (1.00×10^3 kg/m³), and the specific heat capacity of liquid water (4.18×10^3 J/kgK), respectively.

The near surface soil temperature profile, from the surface to the 10 cm depth, is computed from a thermal conductivity equation,

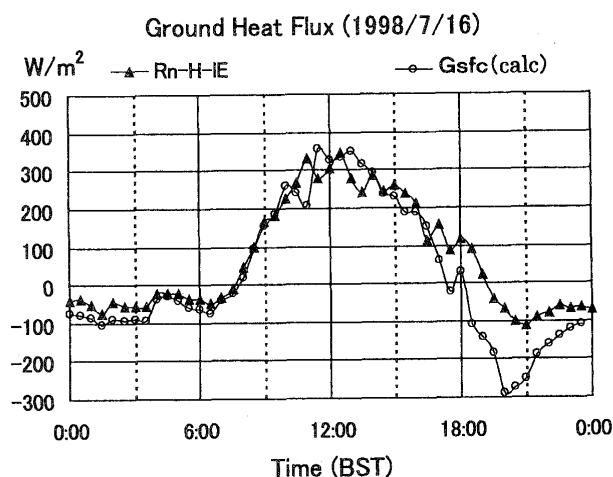


Fig. 10. Comparison of the estimated ground heat flux at surface, G_{sfc} , and the residual flux, $Rn-H-IE$.

$$C_s \frac{\partial T_g}{\partial t} = \frac{\partial}{\partial z} \left(k_s \frac{\partial T_g}{\partial z} \right), \quad (6)$$

where T_g is the soil temperature and k_s the thermal conductivity of soil. The thermal conductivity is parameterized with an empirical function by Al Nakshabandi and Kohnke (1965),

$$k_s = \begin{cases} 419 \exp\{-(P_f + 2.7)\} & P_f \leq 3.1 \\ 0.172 & P_f \geq 3.1 \end{cases} \quad (7)$$

where $P_f = \log_{10} \Psi$, and $\Psi = \Psi_{sat}(\eta/\eta_{sat})$ is moisture potential. The profile of soil water content is given from Soil Moisture and Temperature Mea-

Daily averaged energy fluxes (W/m²)

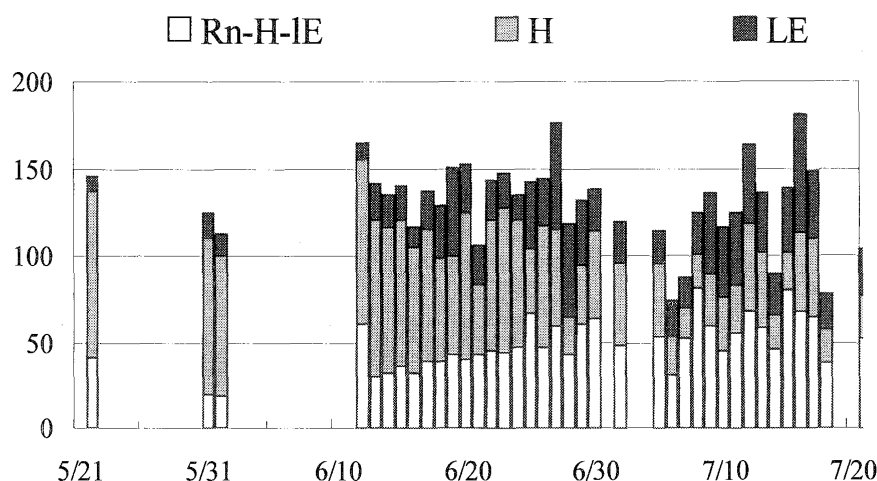


Fig. 11. Surface energy fluxes in daily average. 100 W/m² is equivalent to 8.64 MJ/m²day $Rn-H-IE$: the residual flux from SEB equation. H : the sensible heat flux, LE : the latent heat flux. The total height of three bars show the net radiation flux (Rn).

surement System (SMTMS) moisture data at 4 cm and 20 cm with linear approximation. Unfortunately, soil parameters, η_{sat} , Ψ_{sat} , ρ_d , and c_d are still unknown. Therefore, we used these parameters from United State Department of Agriculture (USDA) (see Table 2) soil data. Although all kinds of soil types except sand and peat were tested, difference of each result was quite small.

The computed G_{sfc} is compared with $Rn-H-lE$ in Figure 10. The calculated soil heat flux fits the residual $Rn-H-lE$ well in the daytime. The maximum value (about 350 W/m²) is also well reproduced. However, from the late afternoon to the midnight, the estimated G_{sfc} falls rapidly. The calculation produces the G_{sfc} as large as -300 W/m² in the minimum (upward), while the residual $Rn-H-lE$ marks about -100 W/m². On the diurnal average, $Rn-H-lE$ is 67.8 W/m² (37.8% of Rn), but G_{sfc} is only 24.0 W/m² (13.2% of Rn). Therefore, there exists 43.8 W/m² (24.6% of Rn) unexplained residual flux on the diurnal average. Although the ambiguous heat storage by near surface soil layer can be explained partially by this estimation, it is not consistent with the energy budget on daily average.

4.3 Daily averaged surface energy budget

The daily averaged surface energy flux during IOP is shown in Figure 11. The bar with dense tone represents the sensible heat flux, the gray tone latent heat flux and the white part the residual. The total height of each bar shows the net radiation.

If we compute a simple arithmetic average of the available daily value from May 21 to July 21, the averaged value of each component is:

$$\left. \begin{array}{l} Rn = 128.3 \\ H = 55.7 \\ lE = 27.0 \\ G_{10\text{ cm}} = 5.7 \end{array} \right\} \quad (\text{W/m}^2)$$

where the $G_{10\text{ cm}}$ is taken from the soil observation. From this averaged data, the residual $Rn-H-lE$ is calculated as

$$Rn - H - lE = 45.6 \quad (\text{W/m}^2).$$

This value is about 36% of the net radiation. On the other hand, the ground heat flux at 10 cm below surface is only 5.7 W/m², which is less than 5% of the net radiation. Thus, unresolved flux reaches more than 30% of the net radiation. If we assume that this unresolved part should be stored in the

near-surface layer, the soil layer needs to be heated by more than 20 °C, which is not observed.

In reference to Eq.(3), the measurement error in net radiation (Rn) is expected to be smaller than that of the other components. Therefore, the unresolved flux, if it is caused by measurement problem, may be attributed to the turbulence flux or soil heat flux. As for the turbulence measurement, the sensible heat flux may be more reliable than the latent heat flux. As seen in Figure 11, the residual increases as the latent heat flux increases. This suggests a possibility of underestimation of latent heat flux.

As for the ground diffusive heat flux, we hereafter will give a bulk estimation of the soil heat flux. The near surface soil layers are frozen during the winter season at the Amdo site. The melting of the soil layer starts in April and proceeds to the deeper layers. The heat flux necessary to feed this melting and the succeeding temperature rise of the soil layers is roughly estimated in the following.

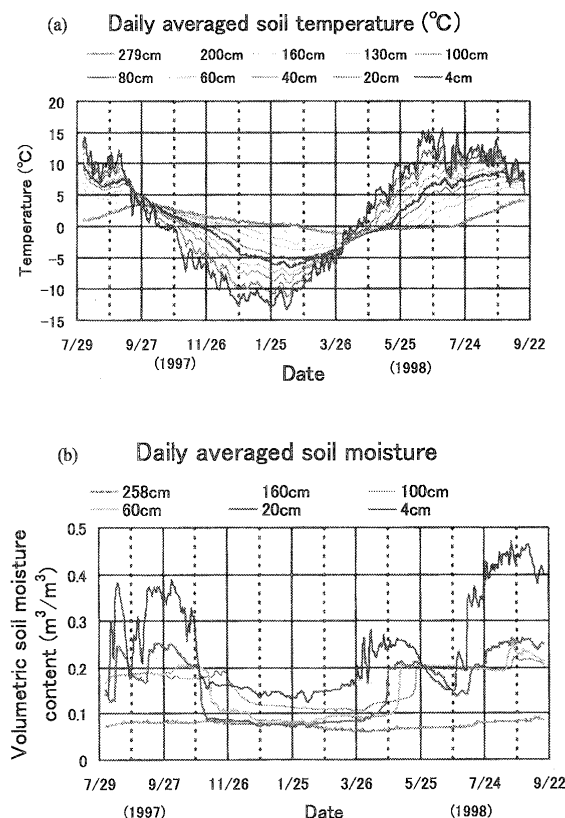


Fig. 12. Daily averaged soil temperature (a) and soil moisture (b). Legends shows the measurement level below surface. Obtained by Soil Moisture and Temperature Measurement System (SMTMS) at Amdo site.

The soil temperature and moisture data are obtained by the SMTMS, installed beside the PBL tower. The system measures soil temperature at 10 depths and soil moisture at 6 depths ranging in 4–279 cm below the surface. Figure 12 shows the 1-day averaged soil moisture and soil temperature. In the record of soil temperature, there exists a period when the temperature stayed near 0 °C in each layer. During this period the soil water was melting and it absorbed the latent heat for fusion. The latent heat for fusion, L_f , is about one-eighth of the latent heat for evaporation, $L_f = 3.38 \times 10^5$ J/kg.

Information on soil water content during the ice phase is necessary. In the ice-phase, the soil moisture sensor (TDR) cannot measure the soil water content correctly. As seen in Figure 12b, the output of the soil moisture sensor suddenly rises when the soil water melts. We assume that the value immediately after the sudden rise of record exhibits the soil water content of the ice-phase. Seeing the record in Fig. 12, we assume the soil moisture content as 20% and estimate the heat capacity as 2.0 MJ/m² using Eq.(7). In addition to this, the following bold assumptions are made for the rough estimation: 1) The heat flux beneath the lowest level is negligible; 2) The soil water began to melt 4/20 at 4 cm, and melting level proceeded downward and reached 279 cm at July 20.

With these assumptions, the latent heat of fusion required to melt the frozen soil water down to 279 cm is estimated as:

$$F = 0.200 \times (2.79 - 0.04) \times \frac{1.00 \times 10^3}{\text{The summed soil water content per unit area}} \times \frac{3.34 \times 10^5}{\text{The latent heat for fusion}} \\ = 1.837 \times 10^8 \text{ (J/m}^2\text{)}$$

Assuming that the melting took place between April 20 to July 20, about 24 W/m² of heat flux is necessary on average. Also, the heat flux needed to heat up the soil layer is roughly estimated as 5 W/m². In total, about 30 W/m² of average heat flux must be transferred to the soil layer from the surface during the period. This value is considerably larger than the observed soil heat flux at 10 cm. If this estimation is valid, a larger part of the unresolved residual in Figure 11 is explained.

5. Conclusion and remarks

At Amdo site on the Tibetan Plateau, an inten-

sive surface layer observation was conducted during May to September 1998 and the following features were revealed.

(1) Each component of the surface radiation flux observed over the plateau had the distinct feature of the optically thin atmosphere. The downward short wave radiation, with little attenuation by the atmosphere, had about 1,100 W/m² at local noon under clear sky condition during summer. Due to the strong surface heating, the surface temperature, and hence the upward long wave radiation, increased rapidly in the daytime, especially in pre-monsoon season. On the other hand, due to the optically thin atmosphere above, the downward long wave radiation was smaller than that observed at a typical sea level site, and the net radiation was not so much greater than low land surrounding the plateau.

(2) During pre-monsoon, the plateau was very dry, with the specific humidity between 2–4 g/kg. The diurnal variation of the surface temperature was as large as 50 °C and the sensible heat flux was dominant. The latent heat flux was as small as 50 W/m² in the diurnal maximum. As the summer monsoon progressed, the surface became wet by frequent precipitation. According to this, diurnal variation of surface temperature reduced to about 20 °C and the share of the latent heat flux increased. The specific humidity increased to 8–10 g/kg.

(3) Detailed data for the diurnal variation of surface fluxes have been obtained, that can be used to validate existing land-atmosphere interaction models and to develop new models.

(4) The surface energy budget was, however, not well closed from the observed data. In terms of the closure ratio, $CR = (H + LE)/(Rn - G)$, the present results shows $CR = 0.7$ and sometimes as low as 0.67. This kind of imbalance has been pointed out by Stannard et al. (1994). He reported that the CR typically ranges between 0.8~0.9 for an agricultural site. Kizer and Elliot (1991) reported a lower value 0.7. Considering the rather sparse vegetation of the site, it is necessary to pursue the cause of imbalance further.

There are various possibilities for this imbalance. One is the underestimation of latent heat flux due to the sensor instability. The sensor of the infrared hygrometer does not work well during and several hours after precipitation. We also showed a bulk estimation of heat transfer to the deeper soil layers needed to melt frozen soil water and heat up the soil layer down to 3 meters. The amount

was enough to explain the residual of surface heat balance. This phenomenon could have significant effect to the surface energy budget, so that the more detailed observational studies are required in future. Besides these instrumentation problems, there exists a discussion that a very weak systematic vertical flow can cause such an imbalance (Lee 1998). Further systematic research is necessary to figure out the cause of flux imbalance.

Acknowledgments

This work has conducted using the data obtained during the Intensive Observation Period in 1998. The observation was conducted in rather tough conditions over the Plateau. The authors would like to express their special thanks to Prof. Jieming Wang of Cold and Arid Regions Environmental and Engineering Research Institute (CARRERI), Chinese Academy of Sciences, for his outstanding coordination throughout the project. Mr. Zeyoung Hu, Mr. Hongchun Gao and other staffs of CARRERI are also acknowledged for their assistance during the observation. The thanks are extended to Prof. Osamu Tsukamoto of Okayama University, Dr. Jun Asanuma at Tsukuba University, Mr. Yongchiao Qi at Ehime University, and other Japanese staffs who engaged in to the boundary layer observation during the IOP. The soil layer data are provided by the courtesy of Prof. Toshio Koike at Tokyo University.

References

- Al Nakshabandi, G. and H. Kohnke, 1965: Thermal conductivity and diffusivity of soils as related to soil moisture tension and other properties, *Agric. For. Meteorol.*, **2**, 271-279.
- Bastiasanssen, W.G.M., 1995: Regionalization of surface flux densities and moisture indicators in composite terrain A remote sensing approach under clear skies in Mediterranean climates. Ph.D. thesis, Agricultural university, 273 pp. [Available from DLO-Staring Centre, P.O. Box 125, 6700 AE Wageningen, the Netherlands]
- Betts, A.K., J. Ball, A.C.M. Beljaars, M.J. Miller, and P.A. Viterbo, 1996: The land surface-atmospheric interaction: a review based on observational and global modeling perspectives, *J. Geophys. Res.*, **101**, 7209-7225.
- and J. Ball, 1998: FIFE Surface Climate and Site-Average Dataset 1987-89, *J. Atmos. Sci.*, **55**, 1091-1108.
- Byun D.W., 1990: On the analytical solutions of flux-profile relationships for the atmospheric surface layer. *J. Appl. Meteorol.*, **29**, 652-657.
- Flohn, H. 1959: Bemerkungen zur Klimatologie von Hochasian. *Abhandlungen der mathematisch-naturwissenschaftlichen klasse*, **14**, 1409-1431
- Chen, L., T. Duan and W. Li, 1985a: Heat source variation and characteristics of energy budget over the Qinghai-Xizhang plateau during the 1979 summer. *Acta Meteorologica Sinica*, **43**, 1-11.
- Clapp, R. and G. Hornberger, 1978: Empirical equations for some soil hydraulic properties. *Water Resour. Res.*, **14**, 601-604.
- Gao, G. and Y. Liu, 1979: a study of the radiation balance, heat balance and heat and cold sources on the earth's surface in eastern Asia. *Scientia Atmospherica Sinica*, **3**, 12-20 [in Chinese].
- Garatt, J.R. 1993: *The Atmospheric Boundary Layer*, Cambridge University press, 312pp.
- Ji, G., Q. Zhong and Z. Shen, 1989: Advances in observation and research of the surface heat source over the Qinghai-Xizang plateau. *Plateau Meteorology*, **5**, 127-132.
- Johnson, D.R., M. Yanai and T.K. Schaak, 1987: Global and regional distributions of atmospheric heat sources and sinks during the GWE. *Monsoon Meteorology*, C.P. Chang, and T.N. Krishnamurti, Eds., Oxford University Press, 271-297.
- Kizer, M.A. and R.L. Elliott, 1991: Eddy correlation systems for measuring evapotranspiration, *Trans. Amer. Soc. Agric. Eng.*, **34**, 387-392.
- Kustas, W.P., J.H. Prueger, K.S. Humes, and P.J. Starks, 1999: Estimation of surface heat fluxes at field scale using surface layer versus mixed-layer atmospheric variables with radiometric temperature observations, *J. Appl. Meteorol.*, **38**, 224-238.
- Lee, X., 1998: On micrometeorological observations of surface-air exchange over tall vegetation, *Agric. For. Meteorol.*, **91**, 39-49.
- Nitta, T. 1983: Observational study of heat sources over the eastern Tibetan Plateau during the summer monsoon. *J. Meteor. Soc. Japan*, **61**, 590-605.
- Noilhan, J. and Planton, 1989: A simple parameterization of land surface processes for meteorological model, *Mon. Wea. Rev.*, **117**, 536-549
- Manabe and Terpsta 1974: The effects of mountains on the general circulation of the atmosphere as identified by numerical experiments. *J. Atmos. Sci.*, **31**, 3-42.
- Pielke R.A., 1984: *The mesoscale meteorological modeling*, Academic press, 612pp.
- Pleim, J.E. and Xiu A., 1995: Development and testing of a surface flux and planetary boundary layer model for application in mesoscale models, *J. Appl. Meteorol.*, **34**, 16-32.
- Satoda H., N. Monji, and Y. Mitsuta, 1985: Energy transfer at the air-ground interface., *Bulletin of DPRI*, Kyoto University, **28**, 415-426.
- Stannard, D.I., J.H. Blanford, W.P. Kustas, W.D.

- Nichols, S.A. Amer, T.J. Schmugge, and M.A. Weltz, 1994: Interpretation of surface flux measurements in heterogeneous terrain during the Monsoon '90 Experiment. *Water Resour. Res.*, **30**, 1227–1239.
- Tamagawa, I., 1994: Turbulent characteristics and bulk transfer coefficients at desert in HEIFE area, *Ph. D. thesis*, Kyoto University.
- , 2000: Considerations on the Eddy Correlation Method Using Sonic Anemometer-Thermometer and Infrared Hygrometer, *J. Japan Soc. Hydrol. & Water Resour.*, **12**, 130–138 (in Japanese).
- and Y. Mitsuta, 1993: Evaporation at desert station in HEIFE, *Proc. of International Symp. on HEIFE*, 379–390.
- Tanaka, K., 1999: Study on the surface energy budget, *M.S. thesis*, Kyoto University (in Japanese).
- van den Hurk, B.J.J.M., Bastiaanssen, W.G.M., Pelgrum, H., and van Meijgaard, E., 1997: A new methodology for assimilation of initial soil moisture fields in weather prediction models using Meteosat and NOAA data, *J. Appl. Meteor.*, **36**, 1271–1283.
- Wang, X. and S. Luo, 1989: The heat source and moisture diagnostic analyses over Tibetan Plateau and its surroundings for May–July 1979. *Plateau Meteorology*, **8**, 13–26 [in Chinese].
- Wang J. and Y. Mitsuta, 1990: Peculiar downward water vapor flux over Gobi desert in the daytime, *J. Meteor. Soc. Japan*, **68**, 399–401.
- Xu, Q. and Qiu, C.-J. 1997: A Variational method for computing surface heat fluxes from ARM surface energy and radiation balance systems. *J. Appl. Meteor.*, **36**, 3–11.
- Yanai, M., Li C. and Song, Z., 1992: Seasonal heating of the Tibetan Plateau and its effect on the evolution of the summer monsoon, *J. Meteor. Soc. Japan*, **70**, 319–351.
- Yeh, T.-C. (Ye, D.), 1988: The thermal structure, convective activity and associated large-scale circulation over the Tibetan Plateau during summer. *Scientia Atmospherica Sinica, Special issue*, 1–12. [In Chinese].
- Zhu, F. and Y. Fan, 1988: Features of diabatic heating and kinetic energy budget over the Qinghai-Xizhang Plateau during early summer 1979. *Acta Meteorologica Sinica*, **2**, 350–359.